

Towards a first-principles determination of effective Coulomb interactions in correlated electron materials: Role of intershell interactions

Priyanka Seth,¹ Philipp Hansmann,^{1,2} Ambroise van Roieghem,^{1,3} Loig Vaugier,¹ and Silke Biermann¹

¹*Centre de Physique Théorique, Ecole Polytechnique, CNRS UMR 7644, 91128 Palaiseau, France*

²*Max-Planck-Institut für Festkörperforschung, Heisenbergstrasse 1, 70569 Stuttgart, Germany*

³*Beijing National Laboratory for Condensed Matter Physics,
and Institute of Physics, Chinese Academy of Sciences, Beijing 100190, China*

(Dated: June 25, 2021)

The determination of the effective Coulomb interactions to be used in low-energy Hamiltonians for materials with strong electronic correlations remains one of the bottlenecks for parameter-free electronic structure calculations. We propose and benchmark a scheme for determining the effective local Coulomb interactions for charge-transfer oxides and related compounds. Intershell interactions between electrons in the correlated shell and ligand orbitals are taken into account in an effective manner, leading to a reduction of the effective local interactions on the correlated shell. Our scheme resolves inconsistencies in the determination of effective interactions as obtained by standard methods for a wide range of materials, and allows for a conceptual understanding of the relation of cluster model and dynamical mean field-based electronic structure calculations.

PACS numbers: 71.15-m,71.27.+a,71.10.Fd

The behavior of electrons in the immediate proximity of the Fermi level determines most of the interesting response properties of materials with strong electronic Coulomb correlations. The *ab initio* derivation of effective Hamiltonians that capture this low-energy physics has therefore become a crucial milestone of modern condensed matter theory, and a prerequisite for materials-specific many-body calculations. While density functional techniques (DFT) [1] provide an established tool to construct the one-body part of the low-energy Hamiltonian, “downfolding” the interaction part is more subtle. The recent development of constrained screening approaches, such as the constrained random phase approximation (cRPA), that identify the interaction parameters to be used in subsequent many-body calculations in a low-energy subspace as matrix elements of partially screened Coulomb interactions [2, 3], have led to tremendous progress, but have also raised new questions. In several systems of recent interest such as atoms adsorbed on surfaces [4, 5] or graphene [6], intersite Coulomb interactions, neglected in the Hubbard model, were found to reach values of up to 50% of the local interactions, triggering work on the inclusion of long-range effects [7–10].

In this Letter, we demonstrate that in prototypical correlated transition metal (TM) oxides and *f*-electron systems, standard calculations omit an even more important additional term, namely intershell interactions that couple the “correlated” shell to itinerant states. Examples are the *d-f* interaction in *f*-electron materials or *d*-ligand interactions in TM oxides. We evaluate these interactions from first principles and derive a scheme to determine *effective intrashell interactions*, which are renormalized by intershell interactions. Our calculations for various materials including Ce, NiO and *f*-electron insulators demonstrate that this “shell-folding scheme” not only fixes present problems in determining effective interactions from first principles, but also gives new insight in how to treat late TM oxides within dynamical mean-field-based (DMFT) techniques [11, 12].

We begin by calculating, using the cRPA implementation of

[3], the interactions between TM 3*d* (or actinide 4*f*) orbitals and O 2*p* ligands to be used in a low-energy Hamiltonian treating both orbital species as correlated. For the actinide oxide UO₂ we find $U^{fp} = 1.9$ eV, as compared to an onsite *f-f* interaction of 6.5 eV and an intersite V^{ff} of 1 eV. For NiO, $U^{dp} = 2.2$ eV still exceeds 25% of the onsite $U^{dd} = 8.6$ eV, and is larger than $V^{dd} = 1.5$ eV. These findings might explain the difficulties that DMFT-based electronic structure calculations face when dealing with late TM oxides [11–13] using a Hamiltonian in which intershell interactions are neglected. Specifically, for NiO, it has been demonstrated that none of the standard double counting correction forms provide spectral properties in agreement with experiment [13]. The situation is similar for rare-earth nickelates and high- T_c cuprates for which intershell *d-p* interaction effects have either been mimicked by adjustable shifts [14, 15] or been taken on a static mean-field level [16].

Electronic structure calculations for elemental cerium usually assume a Hubbard U of the order of 5–6 eV to be applied to the *f*-states. For example, DMFT calculations performed for a low-energy “*f-spdf*” Hamiltonian comprising *s*-, *p*-, *d*- and *f*-states, and a Hubbard correction for the *f*-states of this order of magnitude yield good agreement between theory and a vast body of experimental probes [17–24]. Quite embarrassingly, however, cRPA calculations for an *f-spdf* Hamiltonian, where localized states are constructed for an energy window containing *s*-, *p*-, *d*- and *f*-states but the polarization is constrained to only exclude screening among the *f*-states, give a ridiculously small value (< 1 eV) [25, 26] [27].

We argue here that both considering a second shell as correlated and treating the intershell interaction at least in an effective manner are crucial ingredients to remedy this problem. For α -Ce, assuming *f*- and *d*-states to be correlated within cRPA, we find an intershell interaction $U^{fd} = 1.8$ eV, as compared to $U^{ff} = 6.5$ eV and a negligible intersite $V^{ff} = 0.01$ eV. The large difference in the onsite U^{ff} depending on whether a second shell is treated as correlated (and thus excluded as a screening channel in the cRPA) can

be traced to strong f - spd hybridization. Furthermore, it has been recently argued [2, 28–30] that the effective local Hubbard interaction is a dynamical quantity. The cRPA allows for a direct assessment of this frequency-dependence and its consequences have been intensively studied within DMFT [29, 31–35]. We have calculated $\mathcal{U}(\omega)$ for Ce constructing a Hamiltonian that comprises both $4f$ and $5d$ orbitals as correlated states. The results (see Fig. 1) display a striking similarity in the frequency dependence of U^{ff} , U^{fd} and U^{dd} , and in the magnitude of U^{fd} and U^{dd} , suggesting that screening is dominantly due to the same screening processes (e.g., transitions from f - or d -states to sp -dominated states via strong hybridization as well as plasmon-like excitations). As a consequence, the differences $\tilde{U}^{ff/dd} = U^{ff/dd} - U^{fd}$ are only weakly frequency-dependent quantities. Below, we will argue that these differences acquire a physical meaning as effective interactions when intershell interactions are taken into account in an effective manner.

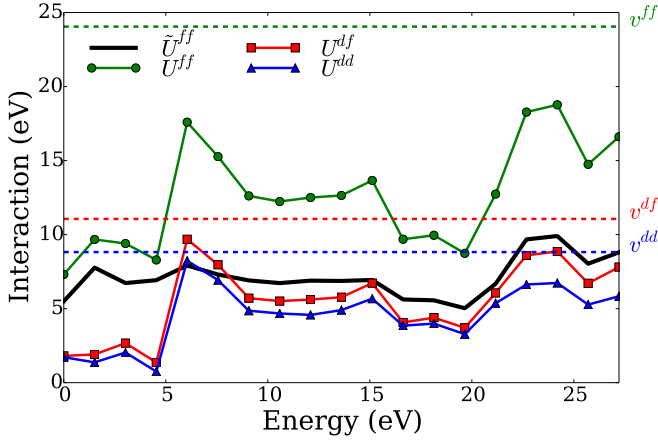


FIG. 1. (Color online) $\mathcal{U}(\omega)$ for df - df and effective (SF) Hamiltonians for cerium.

Consider a multi-orbital Hubbard Hamiltonian for materials where two different orbital shells are treated as correlated. Since, besides Ce, important examples are provided by the TM d - and ligand p -states in TM compounds, we will refer to these two shells as d - and p -shells, with the respective “correlated” and “ligand” subspaces denoted by \mathcal{C} and \mathcal{L} . Our basic assumption is that DFT, within the local density (LDA) or generalized gradient approximation, gives a good estimate for the total energy as a function of the expectation values of the number operators N_d and N_p of the two shells. We further assume that we know the intra- and intershell interactions U^{dd} , U^{pp} , and U^{dp} . In practice, we obtain those from the standard cRPA by suppressing *all* screening channels within the full $\mathcal{C}+\mathcal{L}$ space. Following the spirit of “LDA++” [36, 37], we can then define a *bare* one-body Hamiltonian H_0 as the LDA estimate from which the average interactions within the d - and p -shells have been subtracted. Our multi-orbital Hubbard Hamiltonian now reads: $H = H_0 + H_{\text{int}} - \mu N_{\text{tot}}$, where $H_{\text{int}} = \sum_{\mathbf{R}} h_{\mathbf{R}}$ becomes a sum over the positions \mathbf{R} of the atoms carrying the correlated shell, comprising intra- and in-

tershell Hubbard terms:

$$h_{\mathbf{R}} = \frac{1}{2} \sum_{\substack{(m\sigma) \neq (m'\sigma') \\ m, m' \in \mathcal{C}}} U_{m\sigma m'\sigma'}^{dd} n_{m\sigma} n_{m'\sigma'} + \frac{1}{2} \sum_{\substack{(m\sigma) \neq (m'\sigma') \\ m, m' \in \mathcal{L}}} U_{m\sigma m'\sigma'}^{pp} n_{m\sigma} n_{m'\sigma'} + \sum_{\sigma, \sigma'} U^{dp} N_{d\sigma} N_{p\sigma'}. \quad (1)$$

Here, $U_{m\sigma m'\sigma'}^{dd}$ and $U_{m\sigma m'\sigma'}^{pp}$ are the spin- and orbital-resolved interaction matrix elements, $N_{(d/p)\sigma} = \sum_{m \in \mathcal{C}/\mathcal{L}} n_{m\sigma}$ and $n_{m\sigma} = c_{m\sigma}^\dagger c_{m\sigma}$. To simplify the notation, we have omitted the \mathbf{R} indices on the operators, and the intershell interactions couple only to the total charge on a given shell. A purely algebraic manipulation allows us to rewrite this Hamiltonian as

$$h_{\mathbf{R}} = \frac{1}{2} \sum_{\substack{(m\sigma) \neq (m'\sigma') \\ m, m' \in \mathcal{C}}} \tilde{U}_{m\sigma m'\sigma'}^{dd} n_{m\sigma} n_{m'\sigma'} + \frac{1}{2} \sum_{\substack{(m\sigma) \neq (m'\sigma') \\ m, m' \in \mathcal{L}}} \tilde{U}_{m\sigma m'\sigma'}^{pp} n_{m\sigma} n_{m'\sigma'} + \frac{U^{dp}}{2} N(N-1), \quad (2)$$

with $N = \sum_{\sigma} (N_{d\sigma} + N_{p\sigma})$ and $\tilde{U}_{m\sigma m'\sigma'} = U_{m\sigma m'\sigma'} - U^{dp}$.

The key observation here is that a Hamiltonian with explicit intershell interactions can be rewritten as a sum of interacting Hamiltonians for the two shells, coupled only through an interaction acting on the total charge. The calculations further simplify if for some reason the interactions on the p -shell can be neglected. The usual argument consists in invoking the nearly-complete filling of this shell, which impedes charge fluctuations and allows replacement of operators n_p by their static mean-field values $\langle n_p \rangle$, but this is difficult to justify in late TM oxides where d - p fluctuations are generally the most efficient screening mechanism, substantially reducing the p -occupations. However, as we will see below, U^{dp} can be comparable in magnitude to the intra-ligand-shell interactions U^{pp} , making the effective interaction $\tilde{U}^{pp} = U^{pp} - U^{dp}$ small. The Hamiltonian then has a d - dp form, with correlated d and non-correlated p electrons, and contains the renormalization of the dd -interactions by the intershell interactions: $\tilde{U}^{dd} = U^{dd} - U^{dp}$. Analogously to “downfolding” in energy space, we refer to this scheme as “shell-folding” (SF).

While very suggestive in the sense of the above interpretation, Eq. (2) involves a certain number of subtleties. First, we have divided the solid into cells centred on atoms carrying correlated shells, and constructed ligand Wannier functions *centred on these correlated atoms*. For the prototypical material NiO, this construction is explicitly discussed in the Supplemental Material [38]. It is similar to what is routinely done in cluster model calculations, where hybridizing cluster ligand orbitals are combinations of neighbouring ligand orbitals that are able, by symmetry considerations, to couple to the correlated orbitals. Akin to a Zhang-Rice-type construction [39], a unitary transformation rotates the original Hamiltonian in ligand-centred p -orbitals basis into a “cell Hamiltonian” expressed in TM-centred ligand Wannier functions. The above p degrees of freedom are to be understood in this sense [40].

Furthermore, we have implicitly assumed that the total particle number *on a given cell* is a conserved quantity: the dominant screening channels involve the immediate neighbour ligands, while long-range processes within the dp -subspace are neglected. This assumption is made in cluster model calculations too, and the success of such calculations can be inferred as an *a posteriori* justification of its validity.

The exact rewriting of the Hamiltonian can be understood in a complementary manner: one can formulate the problem as the quest for an optimal auxiliary system with decoupled correlated shells reproducing as closely as possible the physics of the full system. If the free energy is used as a measure of the quality of the approximation, such an optimal system can be constructed via the Peierls-Feynman-Bogoliubov variational principle. Consider the auxiliary Hamiltonian:

$$\tilde{h}_{\mathbf{R}} = \frac{\tilde{U}^{dd}}{2} \sum_{\substack{(m\sigma) \neq (m'\sigma') \\ m, m' \in \mathcal{C}}} n_{m\sigma} n_{m'\sigma'} + \frac{\tilde{U}^{pp}}{2} \sum_{\substack{(m\sigma) \neq (m'\sigma') \\ m, m' \in \mathcal{L}}} n_{m\sigma} n_{m'\sigma'}.$$

The optimal value of the (for simplicity, spherically- and spin-averaged) interactions \tilde{U}^{dd} and \tilde{U}^{pp} are those that minimize the auxiliary free energy $\tilde{F} = F[\tilde{h}_{\mathbf{R}}] + \langle h_{\mathbf{R}} - \tilde{h}_{\mathbf{R}} \rangle_0$, where $\langle \dots \rangle_0$ refers to the average taken with the auxiliary Hamiltonian, and $h_{\mathbf{R}}$ is given by Eq. 1. From the stationarity condition $\partial \tilde{F} / \partial \tilde{U}^{dd} = 0$ we obtain

$$\tilde{U}^{dd} = U^{dd} + \frac{2U^{dp}D^{dp} + (U^{pp} - \tilde{U}^{pp})D^{pp}}{D^{dd}}, \quad (3)$$

where (for $X, Y = d$ or p)

$$D^{XY} = \frac{\partial}{\partial \tilde{U}^{dd}} \sum_{(i\sigma) \neq (j\sigma')} \langle n_{i\sigma}^X n_{j\sigma'}^Y \rangle_0, \quad (4)$$

and an analogous equation for \tilde{U}^{pp} . The optimal interactions are the solutions of this system of equations. If, in addition, we assume that $N = N_d + N_p$ is invariant with respect to changes in $\tilde{U}^{dd/pp}$, these solutions simplify to $\tilde{U}^{dd} = U^{dd} - U^{dp}$ and $\tilde{U}^{pp} = U^{pp} - U^{dp}$, in agreement with Eq. (2) [38]. This requirement imposes that charge may be displaced from the correlated site to the ligand orbitals within the cluster as a result of changes in the interaction, which is equivalent to our assumption that screening takes dominantly place within the immediate neighbourhood of a given atom. Imposing the requirement that increasing the interaction strength only results in charge flow from a site to its nearest neighbours in the single-orbital extended Hubbard model (that is, in an effective Hamiltonian with local and intersite interactions), gives rise to an analogous result as derived in [6]. In this case the effective interaction becomes $\tilde{U} = U - V_{nn}$, where V_{nn} is the nearest-neighbour interaction. Here, a multi-orbital model with two correlated shells and intershell interactions is mapped onto a model with reduced intrashell interactions only and a coupling only to the total charge on a cell, or if $U^{pp} - U^{dp}$ can also be neglected, onto a model with only one correlated shell.

We now discuss how the above shell-folding scheme resolves contradictions arising in modeling specific materials. For α -Ce, our SF scheme finds $F^0 = 4.7$ eV, giving $U^{ff} =$

TABLE I. Slater integrals for correlated shells, average intraorbital U^{pp} for ligand p -shells and intershell $U^{dp/fp}$ for (a) Ce for f - $spdf$, df - df , $spdf$ - $spdf$, (b) NiO and actinide oxides for d - dp , dp - dp , f - fp , fp - fp , and SF models as appropriate. All values in eV.

Ce	f - $spdf$		df - df		$spdf$ - $spdf$				
	f - f	d - d	f - f	d - d	d - d	p - p	s - s		
F^0	0.9	6.5	1.5	7.9	1.8	1.0	0.9		
F^2	5.8	8.8	2.7	9.4	3.1	3.8			
F^4	5.6	6.4	2.5	6.5	2.6				
F^6	4.7	5.1		5.1					
U^{fd}			1.8		2.4				
NiO	d - dp		f - f		f - fp		PuO ₂	CmO ₂	
	dp - dp	SF	f - f	f - fp	SF	SF			
F^0	6.1	8.6	6.4	3.5	3.9	6.5	4.6	5.3	5.9
F^2	9.7	10.1	10.1	5.3	5.8	6.2	6.2	7.3	8.1
F^4	6.6	6.8	6.8	4.3	4.9	5.0	5.0	5.6	6.1
F^6				3.9	4.1	4.2	4.2	4.4	4.8
U^{pp}		6.8	4.6			6.0	4.1	4.3	4.6
$U^{dp/fp}$		2.2				1.9		(2.0)	(2.1)

5.4 eV. This corresponds to the value usually used for cerium. More interestingly, the intrashell interactions $U^{dd} = 1.8$ eV for the d -orbitals are by the same mechanism renormalized to $\tilde{U}^{dd} = 0$, since the intershell interaction equals the initial d - d interaction within numerical accuracy, see Fig. 1 at $\omega = 0$. This justifies the construction of the Hamiltonian for DMFT calculations for cerium, and in particular to the fact that only f -states are treated as correlated. Furthermore, they reconcile the cRPA values with $U \sim 5 - 6$ eV needed in practice.

For paramagnetic NiO, the F^0 for the correlated d -subspace in the SF Hamiltonian (see Table I) is found to be larger than that calculated within the d - dp setup. Extensive cluster model calculations exist for this compound, where interaction strengths have been adjusted so as to reproduce experimental spectra. These optimal values coincide with our calculations within numerical accuracy: Ref. 41 uses $F^0 = 6.5$ eV and finds excellent agreement with experiment (see Fig. 3 in Ref. 41).

The fluorite structure actinide oxides UO₂, PuO₂, and CmO₂ are insulating f -electron compounds that we consider in their non- or paramagnetic phases [38]. In particular, UO₂ has received much interest given its role as a nuclear fuel, and its electronic structure has been studied extensively [45–48]. We have calculated the interactions corresponding to f - f , f - fp and fp - fp Hamiltonians for UO₂. The Slater integrals F^k needed to parametrize these interactions are given in Table I. The increased localization of the f -orbitals in the f - fp model relative to the f - f model is reflected in the larger values of F^k . The magnitude of f - f interactions in UO₂ is significantly larger in the fp - fp model, signaling the importance of p -to- f screening transitions. While integration of the intershell interactions reduces F^0 to the SF value of 4.6 eV, this value remains larger than that obtained in the f -only models. As we proceed along the actinide series, the value of the f - f interaction F^0 in the f - fp model decreases from 3.9 (UO₂) to 3.5 (PuO₂) to 3.4 eV (CmO₂). The increased screening efficiency of the O $2p$ -states as the charge-transfer gap shrinks outweighs the decreased f -orbital extension as the nuclear charge increases. In contrast, the SF F^0 increases from 4.6 (UO₂) to 5.3 (PuO₂) to 5.9 eV (CmO₂). In this case, transitions between p - and f -states do not contribute to the po-

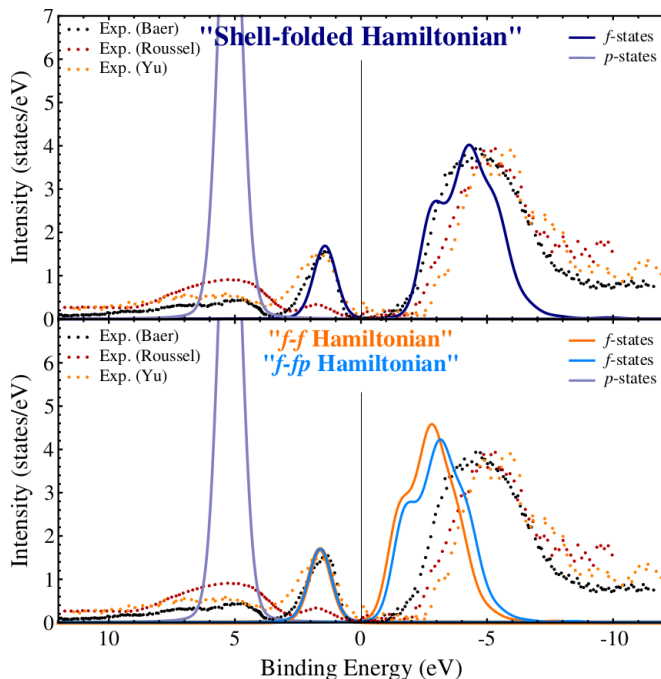


FIG. 2. (Color online) PES and IPES spectra for UO_2 using interaction parameters obtained in the f - f , f - f p and SF models compared to experimental spectra [42–44].

larization, and the increased localization of $5f$ states determines the overall trend. For UO_2 , the p - f charge-transfer energy calculated from the local part of the DFT Hamiltonian, $\Delta = 5.2$ eV, is larger than the $\tilde{U}^{ff} = 4.6$ eV indicating the Mott-Hubbard character of the gap in UO_2 (opening between f -dominated states). On the other hand, PuO_2 and CmO_2 , which respectively have $\Delta = 4.2$ and 3.4 eV, are found to be charge-transfer insulators, with a gap between f - and p -states, in agreement with Ref. 48. With our cRPA results we have performed simulations of (inverse-) photoemission experiments using a configuration-interaction cluster model including the atomic-multiplet theory [49–51] for UO_2 [38]. The spectra obtained using parameters from the f - f , f - f p and shell-folded f p - f p models are compared to experiments in Fig. 2. The gap between the PES and IPES peaks is largely determined by U^{ff} (given the classification of UO_2 as a Mott-Hubbard insulator) and is therefore sensitive to the value of F^0 . Clearly, the calculations both within the f - f and f - f p Hamiltonians severely underestimate the gap. The SF model F^0 matches the experimental estimate of 4.6 ± 0.8 eV to numerical precision [42] and yields spectra in excellent agreement with experiments [52].

In summary, we have presented a scheme for a first-principles determination of the effective Coulomb interactions for materials where ligand-to-correlated-shell hybridizations and interactions cannot be neglected. In the simplest version, intrashell interactions are reduced by the intershell ones, and this estimate provides a remarkably good description of our test materials. Our scheme cures ambiguities in current cRPA calculations in the case of entangled band structures. Finally, our work builds a connection between cluster model calculations, highly successful for spectroscopies of strongly

correlated late TM oxides, and techniques such as DMFT and its extensions treating the solid by embedding an effective local problem into an auxiliary bath.

We thank M. Haverkort for making his cluster calculation package [53] available to us and useful discussions. This work was supported by the Chaire Energies Durables financed by EDF, by IDRIS/GENCI under project 091393, by the French National Research Agency (ANR) grant ANR-10-LABX-0039, and a Consolidator grant of the European Research Council (project 617196).

- [1] W. Kohn, *Rev. Mod. Phys.* **71**, 1253 (1999).
- [2] F. Aryasetiawan, M. Imada, A. Georges, G. Kotliar, S. Biermann, and A. I. Lichtenstein, *Phys. Rev. B* **70**, 195104 (2004).
- [3] L. Vaugier, H. Jiang, and S. Biermann, *Phys. Rev. B* **86**, 165105 (2012).
- [4] P. Hansmann, T. Ayrál, L. Vaugier, P. Werner, and S. Biermann, *Phys. Rev. Lett.* **110**, 166401 (2013).
- [5] P. Hansmann, L. Vaugier, H. Jiang, and S. Biermann, *J. Phys.: Condens. Mat.* **25**, 094005 (2013).
- [6] M. Schüler, M. Rösner, T. O. Wehling, A. I. Lichtenstein, and M. I. Katsnelson, *Phys. Rev. Lett.* **111**, 036601 (2013).
- [7] T. Ayrál, P. Werner, and S. Biermann, *Phys. Rev. Lett.* **109**, 226401 (2012).
- [8] T. Ayrál, S. Biermann, and P. Werner, *Phys. Rev. B* **87**, 125149 (2013).
- [9] L. Huang, T. Ayrál, S. Biermann, and P. Werner, *Phys. Rev. B* **90**, 195114 (2014).
- [10] S. Mahmoudian, L. Rademaker, A. Ralko, S. Fratini, and V. Dobrosavljević, *Phys. Rev. Lett.* **115**, 025701 (2015).
- [11] X. Wang, M. J. Han, L. de’ Medici, H. Park, C. A. Marianetti, and A. J. Millis, *Phys. Rev. B* **86**, 195136 (2012); M. J. Han, X. Wang, C. A. Marianetti, and A. J. Millis, *Phys. Rev. Lett.* **107**, 206804 (2011).
- [12] K. Haule, T. Birol, and G. Kotliar, *Phys. Rev. B* **90**, 075136 (2014).
- [13] M. Karolak, G. Ulm, T. Wehling, V. Mazurenko, A. Poteryaev, and A. Lichtenstein, *J. Electron Spectrosc. Relat. Phenom.* **181**, 11 (2010).
- [14] P. R. C. Kent, T. Saha-Dasgupta, O. Jepsen, O. K. Andersen, A. Macridin, T. A. Maier, M. Jarrell, and T. C. Schulthess, *Phys. Rev. B* **78**, 035132 (2008).
- [15] C. Weber, K. Haule, and G. Kotliar, *Phys. Rev. B* **78**, 134519 (2008).
- [16] P. Hansmann, N. Parragh, A. Toschi, G. Sangiovanni, and K. Held, *New J. Phys.* **16**, 033009 (2014).
- [17] K. Held, A. K. McMahan, and R. T. Scalettar, *Phys. Rev. Lett.* **87**, 276404 (2001).
- [18] M. B. Zöfl, I. A. Nekrasov, T. Pruschke, V. I. Anisimov, and J. Keller, *Phys. Rev. Lett.* **87**, 276403 (2001).
- [19] K. Haule, V. Oudovenko, S. Y. Savrasov, and G. Kotliar, *Phys. Rev. Lett.* **94**, 036401 (2005).
- [20] B. Amadon, S. Biermann, A. Georges, and F. Aryasetiawan, *Phys. Rev. Lett.* **96**, 066402 (2006).
- [21] S. V. Streltsov, E. Gull, A. O. Shorikov, M. Troyer, V. I. Anisimov, and P. Werner, *Phys. Rev. B* **85**, 195109 (2012).
- [22] J. Bieder and B. Amadon, *Phys. Rev. B* **89**, 195132 (2014).
- [23] N. Lanatà, Y.-X. Yao, C.-Z. Wang, K.-M. Ho, and G. Kotliar, *Phys. Rev. B* **90**, 161104 (2014).
- [24] B. Chakrabarti, M. E. Pezzoli, G. Sordi, K. Haule, and G. Kotliar, *Phys. Rev. B* **89**, 125113 (2014).
- [25] F. Aryasetiawan, in *The LDA+DMFT approach to strongly cor-*

- related materials*, edited by E. Pavarini, E. Koch, D. Vollhardt, and A. I. Liechtenstein (Forschungszentrum Jülich GmbH Zentralbibliothek, Verlag, 2011).
- [26] B. Amadon, T. Applencourt, and F. Bruneval, *Phys. Rev. B* **89**, 125110 (2014).
- [27] Interestingly, even when additional screening processes are cut out, corresponding e.g., to transitions involving the Ce- t_{2g} states [26], or when the hybridization is effectively reduced by using a disentangled band structure [54], obtained U values remain on the small side.
- [28] M. Springer and F. Aryasetiawan, *Phys. Rev. B* **57**, 4364 (1998).
- [29] M. Casula, A. Rubtsov, and S. Biermann, *Phys. Rev. B* **85**, 035115 (2012).
- [30] S. Biermann, *J. Phys.: Condens. Mat.* **26**, 173202 (2014).
- [31] P. Werner, M. Casula, T. Miyake, F. Aryasetiawan, A. J. Millis, and S. Biermann, *Nat. Phys.* **8**, 331 (2012).
- [32] L. Huang and Y. Wang, *Europhys. Lett.* **99**, 67003 (2012).
- [33] M. Casula, P. Werner, L. Vaugier, F. Aryasetiawan, T. Miyake, A. J. Millis, and S. Biermann, *Phys. Rev. Lett.* **109**, 126408 (2012).
- [34] A. van Roekeghem, T. Ayril, J. M. Tomczak, M. Casula, N. Xu, H. Ding, M. Ferrero, O. Parcollet, H. Jiang, and S. Biermann, *Phys. Rev. Lett.* **113**, 266403 (2014).
- [35] I. S. Krivenko and S. Biermann, *Phys. Rev. B* **91**, 155149 (2015).
- [36] A. I. Liechtenstein and M. I. Katsnelson, *Phys. Rev. B* **57**, 6884 (1998).
- [37] V. I. Anisimov, F. Aryasetiawan, and A. I. Liechtenstein, *J. Phys.: Condens. Mat.* **9**, 767 (1997).
- [38] See Supplemental Material at [URL] for further details.
- [39] F. C. Zhang and T. M. Rice, *Phys. Rev. B* **37**, 3759 (1988).
- [40] The effective p - d interaction U^{dp} in this basis can be expressed in terms of U^{dp} in the ligand-centred basis, and it has been shown [55] that the two coincide up to a numerical prefactor that is close to 1. For the sake of simplicity, we assume the prefactor to be equal to 1 here.
- [41] T. Hauptrecht, J. Weinen, A. Tanaka, R. Gierth, S. G. Altendorf, Y.-Y. Chin, T. Willers, J. Gegner, H. Fujiwara, F. Strigari, A. Hendricks, D. Regesch, Z. Hu, H. Wu, K.-D. Tsuei, Y. F. Liao, H. H. Hsieh, H.-J. Lin, C. T. Chen, and L. H. Tjeng, (2012).
- [42] Y. Baer and J. Schoenes, *Solid State Commun.* **33**, 885 (1980).
- [43] P. Roussel, P. Morrall, and S. Tull, *J. Nucl. Mater.* **385**, 53 (2009).
- [44] S.-W. Yu, J. G. Tobin, J. C. Crowhurst, S. Sharma, J. K. Dewhurst, P. Olalde-Velasco, W. L. Yang, and W. J. Siekhaus, *Phys. Rev. B* **83**, 165102 (2011).
- [45] B. Dorado, B. Amadon, M. Freyss, and M. Bertolus, *Phys. Rev. B* **79**, 235125 (2009).
- [46] Q. Yin and S. Y. Savrasov, *Phys. Rev. Lett.* **100**, 225504 (2008).
- [47] Q. Yin, A. Kutepov, K. Haule, G. Kotliar, S. Y. Savrasov, and W. E. Pickett, *Phys. Rev. B* **84**, 195111 (2011).
- [48] X.-D. Wen, R. L. Martin, T. M. Henderson, and G. E. Scuseria, *Chem. Rev.* **113**, 1063 (2013).
- [49] A. Tanaka and T. Jo, *J. Phys. Soc. Jpn* **63**, 2788 (1994).
- [50] F. de Groot, *J. Electron Spectrosc. Relat. Phenom.* **67**, 529 (1994).
- [51] T. T. M. Issue, *J. Electron Spectrosc. Relat. Phenom.* **86** (1997).
- [52] The variation in the experimental spectra is likely due to differences in determination of the chemical potential. To match our cluster spectra intensity, the BIS spectra by Baer and Schoenes [42] were scaled 2.5x, close to the factor of 2 suggested in their paper based on normalization considerations.
- [53] M. W. Haverkort, M. Zwierzycki, and O. K. Andersen, *Phys. Rev. B* **85**, 165113 (2012).
- [54] F. Nilsson, R. Sakuma, and F. Aryasetiawan, *Phys. Rev. B* **88**, 125123 (2013).
- [55] L. F. Feiner, J. H. Jefferson, and R. Raimondi, *Phys. Rev. B* **53**, 8751 (1996).

Towards a first-principles determination of effective Coulomb interactions in correlated electron materials: Role of intershell interactions – Supplementary Material

In this supplementary material, we provide a brief review of the constrained random phase approximation, additional background on our benchmark materials and further details on the computations presented in the main part of the paper. We end with a discussion relating our findings to current electronic structure approaches.

CONSTRAINED RANDOM PHASE APPROXIMATION

The constrained random phase approximation as proposed in [S1] has allowed for the first principles determination of the effective local Coulomb interaction, the “Hubbard U ”, that is used as the bare interaction in a low-energy Hamiltonian for a wide range of correlated materials ranging from transition metals [S1–S4], their oxides [S5–S10], pnictides and chalcogenides [S11–S16], f -electron materials [S17–S19] to organic conductors [S20, S21] and solid hydrogen [S22]. Probably the most important advantage of cRPA over previous methods such as the constrained LDA [S23–S25] or linear response [S26] schemes is the possibility of adapting U to the chosen low-energy model. For reviews, see [S14, S27, S28].

The underlying idea of the constrained random phase approximation is the observation that the Hubbard U should be obtained as the matrix element of a *partially-screened* interaction in some localized basis. This partially-screened interaction is constructed such that screening at the RPA level calculated for the low-energy Hamiltonian or for the full Coulomb Hamiltonian lead to the same result for the fully-screened Coulomb interaction.

Mathematically, this can be obtained by constructing a partial polarization function where certain screening processes are suppressed: $P_r = P - P_d$, where P_d is the polarization within the low-energy space, which at the RPA level is a sum over particle-hole transitions that take entirely place within the low-energy subspace. The partially-screened interaction is then obtained as $W_r = v/(1 - P_r v)$ where v is the bare Coulomb interaction. Finally, the matrix of Hubbard interactions $U_{mm'm''m'''}$ is obtained as matrix elements of W_r within the basis of localized Wannier functions used for the construction of the Hamiltonian.

Subtleties arise when one aims at constructing a multi-orbital Hamiltonian which comprises more orbital degrees of freedom at the one-particle level than in its interacting part. The commonly applied strategy [S13] in this case is to construct Wannier functions for all orbitals, but exclude screening transitions corresponding to the interacting degrees of freedom only. However, ambiguities arise in this case when the correlated bands are entangled with itinerant ones. Several disentanglement strategies have been proposed [S2, S19], but it may appear somewhat unsatisfactory to deal with effectively an altered one-particle band structure, in particular since by construction, the stronger the entanglement, the larger the deviations. Alternatively, one may think that in these cases it could be advisable to rather reconsider the philosophy of cut-

ting out only the few correlated states out of a bigger number of entangled states living roughly at the same energy. Our work presents a well-defined solution following this philosophy.

BACKGROUND ON THE BENCHMARK COMPOUNDS

Cerium

Elemental cerium has intrigued the solid state community for decades due to its isostructural volume-collapse transition. This “ α - γ ” transition is of first order below a critical temperature $T_c = 600\text{K}$, and ends in a second-order critical point at T_c . At room temperature the decrease in volume when going from the γ to the α phase is as large as 15%. A Curie-Weiss magnetic susceptibility in the γ phase signals the presence of localized $4f$ electrons that delocalize in the α phase where the magnetic susceptibility becomes Pauli-like. In this phase, the $4f$ electrons participate in the bonding (resulting in the smaller volume) and the formation of quasiparticles, as seen in photoemission [S29, S30].

The origin of this transition has been the subject of intense debate in the literature. The “Mott transition picture” interprets it as a delocalization-localization transition in the $4f$ shell only [S31]. The “Kondo volume collapse” (KVC) picture [S32–S34] in contrast attributes the leading role to the hybridization between the $4f$ electrons and (spd -) itinerant states: the stronger hybridization in the α -phase leads to a high Kondo temperature and thus to screening of the $4f$ local moment, while the high-volume γ -phase has a low Kondo temperature, leading in practice to unscreened moments at intermediate temperatures.

Cerium has long served as a test material for methods that go beyond the LDA [S35, S36] and in particular for DMFT-based electronic structure calculations [S37–S46]. Combined DFT+DMFT was found to be able to disentangle subtle electronic-structure changes in the hybridization to elucidate the mechanism of the transition, and give a description of spectral, optical and magnetic properties in agreement with experiments. It was also emphasized, however, that at any relevant temperature the entropic contribution dominates over the internal energy changes and pressure contribution such that the question of the existence of a double minimum in the internal energy acquires a somewhat academic character. We mention very recent QMC calculations [S47] that advocate the existence of a transition down to zero temperature.

With the advent of more efficient Monte Carlo techniques for the DMFT equations in the multi-orbital case in recent years, the problem has been extensively revisited, and not only total energies, but also entropy and free energy have been computed [S44]. Recent work has also focused on the role of spin-orbit coupling [S45, S48].

While many-body calculations for cerium have thus been extremely successful, U values have generally been used as

adjustable parameters, and several authors have discussed the difficulties in determining the effective Hubbard interactions from first principles. This comes without surprise since this material can be considered a “worst-case” scenario, precisely due to the strong hybridization of the $4f$ -states with itinerant conduction band states present at the same energy. Ref. S49 has presented a detailed study of various choices of low-energy models, arriving at the conclusion that any low-energy Hamiltonian of f - $spdf$ type would have U^{ff} -values lower than 1 eV in cRPA. This illustrates the problem: there is a clear consensus in the literature that a much larger value of 5 to 6 eV is necessary to reproduce the available experimental findings. Nilsson et al. [S19] proposed a disentanglement scheme which, by essentially replacing the original band structure by an approximate one with reduced hybridization, yields larger (though still too small) values of 4.3 eV and 5.4 eV for α and γ cerium respectively.

NiO

NiO has been put forward as a challenge to solid state theory and electronic structure calculations since the very early days: Mott highlighted the inadequacies of the band picture in describing the physics of this compound. NiO is an antiferromagnetic insulator below a Néel temperature of 525 K. Above T_N , the antiferromagnetic order disappears, but the material remains insulating with a large gap of 4 eV that largely exceeds the energy scale of the Néel temperature). Furthermore, its spectral properties are remarkably insensitive to the presence or absence of magnetic order. This calls for a theoretical description of the insulating nature without relying on magnetic order.

The story became more involved with the seminal work of Zaanen, Sawatzky and Allen [S50], who distinguished between Mott insulators where the gap opens due to the Coulomb blocking between correlated states of the same shell character, and charge-transfer insulators where the Hubbard interactions are larger than the O $2p$ to Ni $3d$ charge-transfer energy such that the first ionization states are in fact of O p character.

In NiO, it was already known that a satellite feature at -8 eV binding energy is mainly of d character, while the low-energy states at the Fermi level have large oxygen $2p$ character. A series of photoemission (including resonant photoemission) works elucidated the different transitions in detail [S51–S60].

NiO was treated within many-body perturbation theory within the GW approximation by Aryasetiawan and Gunnarsson [S61]. The authors found the gap to open within this approximation, but also pointed out failures concerning the gap character which remains Mott-Hubbard like, and satellite structures related to the strongly-atomic character of the $3d$ states.

The first DMFT works on NiO used a Hamiltonian where only the TM $3d$ states were included [S62]. Soon thereafter, it was pointed out that this was questionable due to the d -ligand interplay at the Fermi level. Several subsequent works included ligand states as itinerant states in the one-body Hamil-

tonian [S63, S64]. However, none of the standard double counting corrections appeared to be appropriate in this case [S65], and NiO still appears to be a challenge to DMFT-based or DMFT-like theories [S66].

Actinide oxides: UO_2 , PuO_2 and NpO_2

The actinide dioxides UO_2 , PuO_2 and NpO_2 are insulating materials with similar gaps (of 2.1 eV [S67], 2.9 eV [S68] and 2.8 eV [S68] respectively, but quite different ground states. UO_2 has been and remains the subject of intense interest from the applied materials perspective thanks to its application as a nuclear fuel. Electronic structure calculations thus focus not only on questions of stability of different structures, but also attempt to assess the physics of impurities resulting from the radioactive decay processes. We mention for example the study of He atom incorporation into UO_2 crystals by [S69], where LDA+U with $U = 4.6$ eV was employed. For an extensive review and recent work see [S70]. Interestingly, corrections to simple DFT-LDA calculations turn out to be necessary not only for the description of spectral properties but even in assessing the energetics, and UO_2 has become a playground for electronic structure approaches. While the value of U has typically been considered an adjustable parameter or guessed from spectroscopy experiments, we note that the values employed coincide remarkably well with our results discussed in the main text.

The series of actinide dioxides has also attracted much interest due to their exotic low-temperature (multi-polar) ordered states. While in PuO_2 the f^4 configuration leads to a non-magnetic ground state, UO_2 has a complex antiferromagnetic order below a Néel temperature of 30.8 K [S71], with a transverse 3-k arrangement driven by quadrupolar interactions. NpO_2 on the other hand displays a longitudinal 3-k order below an ordering temperature of 25 K, with a rank-5 magnetic multipole (“triakontadipole”). Despite being difficult due to the noncollinear character of the order and high-rank order parameters, LDA+U calculations are successful in describing the multi-polar order with interaction values of $U = 4$ eV [S72].

Their complex electronic structure has always been considered a challenge also for purely functional-based first-principles calculations, and it is not surprising that the actinide oxides became a playground and tested for hybrid functionals (see e.g., [S73, S74]). A comprehensive review of various electronic structure calculations of the actinide oxides is given in [S71].

DETAILED DERIVATION OF THE SHELL-FOLDED HAMILTONIAN

Here we present the derivation of the shell-folded Hamiltonian by the Peierls-Feynman-Bogoliubov variational principle in a step-by-step manner and determine the form of our effective interactions $\tilde{U}^{dd} = U^{dd} - U^{pd}$ and $\tilde{U}^{pp} = U^{pp} - U^{pd}$.

Consider the dp Hamiltonian

$$h_{\mathbf{R}} = \frac{\tilde{U}^{dd}}{2} \sum_{\substack{(m\sigma) \neq (m'\sigma') \\ m, m' \in \mathcal{C}}} n_{m\sigma} n_{m'\sigma'} + \frac{\tilde{U}^{pp}}{2} \sum_{\substack{(m\sigma) \neq (m'\sigma') \\ m, m' \in \mathcal{L}}} n_{m\sigma} n_{m'\sigma'} \\ + \tilde{U}^{dp} \sum_{\substack{m \in \mathcal{C}, \sigma \\ m' \in \mathcal{L}, \sigma'}} n_{m\sigma} n_{m'\sigma'},$$

and the auxiliary Hamiltonian

$$\tilde{h}_{\mathbf{R}} = \frac{\tilde{U}^{dd}}{2} \sum_{\substack{(m\sigma) \neq (m'\sigma') \\ m, m' \in \mathcal{C}}} n_{m\sigma} n_{m'\sigma'} + \frac{\tilde{U}^{pp}}{2} \sum_{\substack{(m\sigma) \neq (m'\sigma') \\ m, m' \in \mathcal{L}}} n_{m\sigma} n_{m'\sigma'}.$$

where $\tilde{U}^{dd/pp}$ are the effective Coulomb interactions for the d and p manifolds. We find their optimal values by minimizing $\tilde{F} = F[\tilde{h}_{\mathbf{R}}] + \langle h_{\mathbf{R}} - \tilde{h}_{\mathbf{R}} \rangle_0$ with respect to \tilde{U}^{dd} and \tilde{U}^{pp} , where $\langle \dots \rangle_0$ refers to the average taken with the auxiliary Hamiltonian. Let us also extend the definition

$$D_Z^{XY} = \frac{\partial}{\partial \tilde{U}^Z} \sum_{(i\sigma) \neq (j\sigma')} \langle n_{i\sigma}^X n_{j\sigma'}^Y \rangle_0.$$

where $X, Y, Z = d$ or p .

Then, from the stationarity condition $\partial \tilde{F} / \partial \tilde{U}^{dd} = 0$ we obtain

$$\tilde{U}^{dd} = U^{dd} + \frac{2U^{dp} D_d^{dp} + (U^{pp} - \tilde{U}^{pp}) D_d^{pp}}{D_d^{dd}}.$$

and an analogous equation for \tilde{U}^{pp} .

Solving the system of equations, we have for $\Delta = \tilde{U}^{dd} - U^{dd}$,

$$\Delta = \frac{\Delta D_p^{dd} - 2U^{dp} D_p^{dp} D_d^{pp}}{D_p^{pp}} \frac{D_d^{pp}}{D_d^{dd}} + \frac{2U^{dp} D_d^{dp}}{D_d^{dd}}$$

Simplifying this expression gives

$$\frac{\tilde{U}^{dd} - U^{dd}}{U^{pd}} = \frac{2D_d^{pd} D_p^{pp} - 2D_p^{pd} D_d^{pp}}{D_d^{dd} D_p^{pp} - D_p^{dd} D_d^{pp}}.$$

Assuming that the total number of particles is invariant with respect to changes in the effective parameters, namely that

$$\frac{\partial \langle N(N-1) \rangle}{\partial \tilde{U}^{dd}} = \frac{\partial \langle N(N-1) \rangle}{\partial \tilde{U}^{pp}} = 0,$$

or equivalently that

$$D_d^{dd} + 2D_d^{dp} + D_d^{pp} = 0, \\ D_p^{dd} + 2D_p^{dp} + D_p^{pp} = 0,$$

we can simply the above to

$$\frac{\tilde{U}^{dd} - U^{dd}}{U^{pd}} = -1.$$

Thus, we obtain that

$$\tilde{U}^{dd} = U^{dd} - U^{pd}, \\ \tilde{U}^{pp} = U^{pp} - U^{pd}.$$

While the above derivation is presented for spin- and orbital-averaged interactions for simplicity, it is equally applicable to the orbital-resolved interactions $U_{m\sigma m'\sigma'}$. As long as we assume the intershell interaction to be an orbital-independent average U^{dp} , the resulting effective interactions are obtained from an effective reduced Slater integral $\tilde{F}^0 = F^0 - U^{dp}$. Note that quadratic terms H_0 are unchanged. As we are devising an effective model for the *local* $h_{\mathbf{R}}$, and as our summations run explicitly over all orbitals contained therein, we do not have to consider either the number of equivalent atoms within the unit cell or its coordination.

CONSTRUCTION OF TRANSITION METAL CENTRED WANNIER FUNCTIONS

In the principal part of the Letter, we derived a low-energy model that we showed to be successful in treating intershell interactions in addition to the intrashell interactions. Here, using NiO as an example, we describe the construction of the ‘‘ring’’ orbitals centred on the correlated site as a superposition of the ligand p orbitals. This ring orbital construction is inspired by the cell-perturbation methods [S75–S77] that emerged as a consequence of the Zhang-Rice construction [S78] for the Cu superconductors.

NIO

Construction of ring orbitals

NiO adopts the rock-salt structure with a face-centred cubic lattice of Ni atoms intercalated with a face-centred cubic lattice of O atoms. As the conventional unit cell contains four formula units, for simplicity, we choose to work globally in the Cartesian coordinate system with the primitive unit cell vectors

$$\mathbf{a} = (1/2, 1/2, 0), \\ \mathbf{b} = (1/2, 0, 1/2), \\ \mathbf{c} = (0, 1/2, 1/2).$$

Our basis consists of one Ni atom at $(0, 0, 0)$ and one O atom at $(1/2, 1/2, 1/2)$. We define the corresponding k -vectors $\mathbf{k}_{\mathbf{a}}, \mathbf{k}_{\mathbf{b}}, \mathbf{k}_{\mathbf{c}}$ such that $\mathbf{k}_{\mathbf{i}} \cdot \mathbf{j} = 2\pi\delta_{ij}$.

In order to find matrix elements of $H(\mathbf{k})$, we first determine the Ni $3d$ to O $2p$ hopping directions. Using the Slater-Koster parametrization [S79], we write the matrix elements of the real-space tight-binding Hamiltonian $H(\mathbf{R})$ as functions of the p - p , p - d and d - d two-center bond integrals that give the strength of bonding in a given direction, reflecting the relative orbital lobe positions. We use the standard notation of σ -bonding if the lobes point to each other and π -bonding if the lobes are parallel. The resulting matrix is finally Fourier-transformed to $H(\mathbf{k})$ in momentum space. We note that, besides hopping, the cubic crystal field splitting of Ni $3d$ -states into e_g and t_{2g} (parametrized in the usual notation as $10Dq$) is also included in $H(\mathbf{k})$. The final $H(\mathbf{k})$ in matrix form is given

in Table I. The diagonalization of this Hamiltonian yields the tight-binding band structure.

We now construct Ni-centred ring orbitals from the three O $2p$ states. This is similar to what is done in typical cluster calculation ligand orbitals [S80]. The bonding cluster orbitals corresponding to the NiO₆ octahedron are shown in Fig. S1.

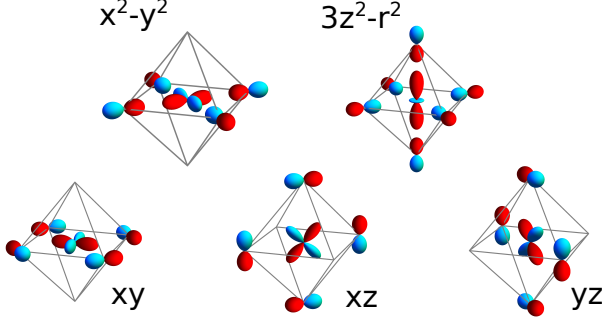


FIG. S1. The NiO₆ octahedron cluster orbitals.

One key difference between our ring orbitals and the cluster orbitals, however, is that the cluster orbitals are constructed entirely in real space from combinations of a finite number of orbitals. In our case, we use a coherent superposition of orbitals on an all (infinite) sites, giving rise to a k -dependence (see the sin terms in Eq. S1). From the three available oxygen states we can construct two e_g -type rings, which locally hybridize with the Ni e_g orbitals and a third, a_{1g} (i.e., s -like) ring which is locally non-bonding with the Ni e_g orbitals. The form of these rings is shown in Fig. S2.

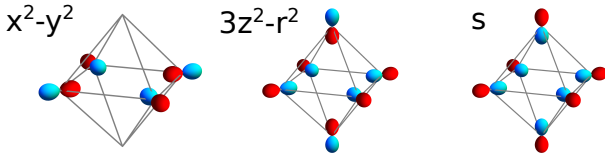


FIG. S2. The NiO ring orbitals. The first two orbitals have e_g symmetry while the last is of a_{1g} symmetry.

Mathematically, we perform a unitary transformation on the $2p$ subspace of the original Hamiltonian H to \tilde{H} by $\tilde{H} = THT^\dagger$. The transformation matrix T takes us from the $(p_x, p_y, p_z, d_{xy}, d_{yz}, d_{xz}, d_{x^2-y^2}, d_{z^2})$ to $(\tilde{p}_{x^2-y^2}, \tilde{p}_{z^2}, \tilde{p}_s, d_{xy}, d_{yz}, d_{xz}, d_{x^2-y^2}, d_{z^2})$ basis, and is given by

$$T = \begin{pmatrix} \frac{s_x}{\sqrt{2}} & -\frac{s_y}{\sqrt{2}} & 0 & 0 & 0 & 0 & 0 & 0 \\ \frac{s_y}{\sqrt{2}} & \frac{s_x}{\sqrt{2}} & \frac{-2s_z}{\sqrt{6}} & 0 & 0 & 0 & 0 & 0 \\ \frac{s_y}{\sqrt{6}} & \frac{s_x}{\sqrt{6}} & \frac{s_z}{\sqrt{6}} & 0 & 0 & 0 & 0 & 0 \\ \frac{s_y}{\sqrt{3}} & \frac{s_x}{\sqrt{3}} & \frac{s_z}{\sqrt{3}} & 0 & 0 & 0 & 0 & 0 \\ 0 & 0 & 0 & 1 & 0 & 0 & 0 & 0 \\ 0 & 0 & 0 & 0 & 1 & 0 & 0 & 0 \\ 0 & 0 & 0 & 0 & 0 & 1 & 0 & 0 \\ 0 & 0 & 0 & 0 & 0 & 0 & 1 & 0 \\ 0 & 0 & 0 & 0 & 0 & 0 & 0 & 1 \end{pmatrix} \quad (\text{S1})$$

TABLE I. The Hamiltonian operator in momentum space, $H(\mathbf{k})$, in the basis $(O 2p_x, O 2p_y, O 2p_z, Ni 3d_{xy}, Ni 3d_{yz}, Ni 3d_{xz}, Ni 3d_{x^2-y^2}, Ni 3d_{z^2})$. To improve readability we employ the abbreviations $s_i = \sin(\frac{k_i}{2})$ and $c_i = \cos(\frac{k_i}{2})$.

$\epsilon_p + 2pp\sigma c_x (c_y + c_z)$	$-2pp\sigma s_x s_y$	$-2ipd\pi s_z$	0	$-2ipd\pi s_z$	$-i\sqrt{3}pd\sigma s_x$	$ipd\sigma s_x$
$-2pp\sigma s_x s_y$	$\epsilon_p + 2pp\sigma (c_x c_y + c_y c_z)$	$-2ipd\pi s_x$	$-2ipd\pi s_z$	0	$i\sqrt{3}pd\sigma s_y$	$ipd\sigma s_y$
$-2pp\sigma s_x s_z$	0	$-2ipd\pi s_y$	0	$-2ipd\pi s_x$	0	$-2ipd\sigma s_z$
$2ipd\pi s_x$	0	$-4Dq + \epsilon_d + 3dd\sigma c_x c_y$	0	0	$\sqrt{3}dd\sigma s_x s_y$	$\sqrt{3}dd\sigma s_x s_y$
0	$2ipd\pi s_z$	0	0	0	0	$-\frac{\sqrt{3}}{2}dd\sigma s_x s_z$
$2ipd\pi s_z$	0	$-4Dq + \epsilon_d + 3dd\sigma c_y c_z$	0	0	$\frac{3}{2}dd\sigma s_y s_z$	$-\frac{\sqrt{3}}{2}dd\sigma s_x s_z$
$i\sqrt{3}pd\sigma s_x$	0	$-\frac{3}{2}dd\sigma s_x s_z$	$-4Dq + \epsilon_d + 3dd\sigma c_x c_z$	0	$-\frac{3}{2}dd\sigma s_x s_z$	$-\frac{\sqrt{3}}{4}dd\sigma (c_x - c_y) c_z$
$-ipd\sigma s_x$	$\sqrt{3}dd\sigma s_x s_y$	$-\frac{\sqrt{3}}{2}dd\sigma s_x s_z$	$-\frac{\sqrt{3}}{2}dd\sigma s_x s_z$	0	$6Dq + \epsilon_d + \frac{1}{4}dd\sigma (c_x c_z + c_y c_z)$	$6Dq + \epsilon_d + \frac{1}{4}dd\sigma (c_y c_z + c_x (4c_y + c_z))$

We have used the abbreviation $s_i = \sin(\frac{k_i}{2})$. The transformation is chosen such that the ring with $d_{x^2-y^2}$ symmetry is exact, while the d_{z^2} and s -like rings are approximate in order to orthogonalize them.

In the original O-centred p basis, the hybridization elements decay with distance as shown in Fig. S3. Note that the distances are measured in conventional lattice units. As we choose to construct a maximally-symmetric primitive cell as described above, the O atoms closest to the Ni atom at (0,0,0) actually lie in the nearest-neighbour unit-cells rather than within the (0,0,0) unit cell. This is reflected in the peak in $t_{t_{2g}p}$ and $t_{e_g p}$ at $(0,0,\frac{1}{2})$. As the d -subspace of the Hamiltonian is untouched by the transformation, the t_{dd} hybridizations in the original p basis and in the ring basis are identical.

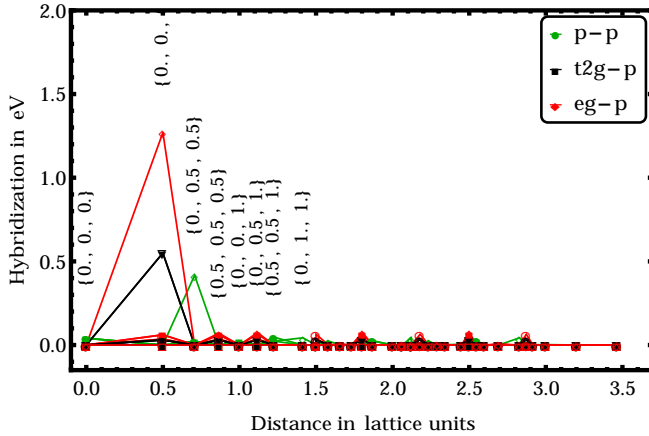


FIG. S3. Matrix elements of the initial dp Hamiltonian $H(\mathbf{k})$ in real space plotted as a function of distance (measured in conventional unit cell lengths).

In the Ni-centred ring basis, the decay of the hybridization elements is plotted in Fig. S4. The s -like ring orbital is always non-bonding locally; however, given that the symmetry of this orbital is not imposed exactly in order to ensure unitarity of the transformation, it continues to hybridize weakly with the Ni d orbitals. For further symmetry reasons, the $d_{x^2-y^2}$ -like ring orbital alternates between being bonding and anti-bonding over second nearest-neighbours.

The transformation of the p orbitals into ring orbitals also modifies the interaction parameters U^{pp} . Notably, the intra-ring interaction decreases as the rings become more delocalized, while inter-ring interactions increase as overlap between orbitals increases. The ring- d interactions are unchanged due to symmetry reasons.

UO2

In Fig. S5, we show the 7 bonding ligand orbitals for the eight-fold coordinated U $5f$ states. We can construct ligand orbitals by linear combination of O $2p$ states matching the respective symmetry of the U $5f$ orbitals as was done for NiO above. However, unlike for a finite size cluster, we cannot create Bloch states associated to each of the ligand orbitals (in the unit cell we have only six oxygen states). Hence, in order

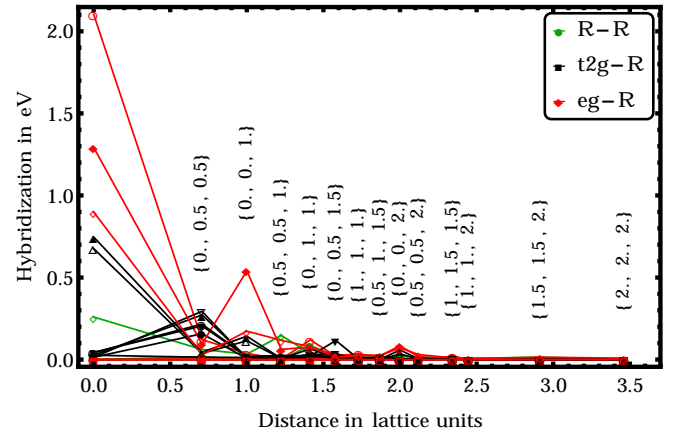


FIG. S4. Matrix elements of the transformed d -ring Hamiltonian $\tilde{H}(\mathbf{k})$ in real space plotted as a function of distance (measured in conventional unit cell lengths).

to construct ring-orbitals one has to choose which six basis states to include, as in NiO.

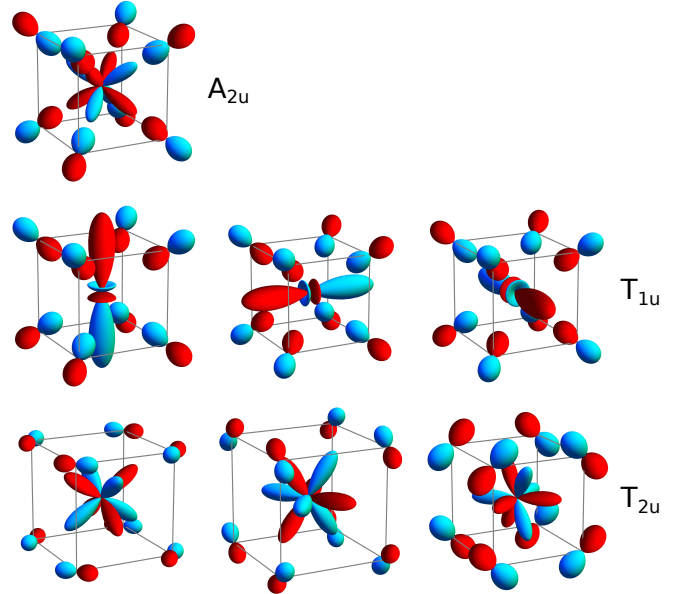


FIG. S5. The 7 bonding ligand orbitals constructed as linear combinations of the 8 p orbitals with the symmetry of the corresponding f orbital.

Finally, we give the computational details for the cluster model calculations for UO_2 that result in the spectral functions shown in Fig. 2 of the main text. In the calculation, both f - and p -states, separated by the charge-transfer energy given by LDA, are included but are not allowed to hybridize. The parameters used for the UO_2 cluster model are $E_{a_u} = 0.349$, $E_{t_{1u}} = -0.039$, $E_{t_{2u}} = -0.077$, $\Delta_{fp} = 5.189$, which were obtained from LDA and $\zeta_{5f} = 0.27$, obtained from an atomic HF calculation. The hybridization parameters $V(a_u) = V(t_{1u}) = V(t_{2u}) = 0$. All values are in eV.

OVERVIEW OF U VALUES USED IN THE LITERATURE

TABLE II. Screened Coulomb interactions used in the literature. All values in eV.

Interaction parameters		References
$U = 4.5$	$J = 0.51$	S81–S83
$\bar{U} = 4.5$		S84
$\bar{U} = 4.5$	$\bar{J} = 0.51$	S85
$U = 4.5$	$J = 0.54$	S86
$U = 4.6$	$J = 0.5$	S87
$U = 7.7$		S88
$U = 4.0$	$J = 0.51$	S89
$U = 4.5$	$J = 0.5$	S90
$U = 3.0, 6.5$	$J = 0.7$	S91
$U = 4.5 - 4.75$	$J = 0.54$	S92
$U = 4.0$		S93
$U = 8.0$		S94
$U = 6.0$	$J = 0.5 - 0.6$	S95
$U = 3.0$		S96
$U = 4.0$	$J = 0 - 0.5$	S97

In Table II we present an overview of Hubbard U values used for calculations for UO_2 in the literature. It is remarkable how close most of these values are to the result of our shell-folded theory.

Nevertheless, a recent work by Kolorenč *et al.* [S91] presented LDA+DMFT calculations using a larger value of $F^0 = 6.5\text{eV}$. The authors show that the observed spectral function closely resembles spectra calculated within the Hubbard I approximation using a smaller U of 3 eV. Apart from a satellite structure at about 10 eV, the spectral features between these two theories presented an impressive match. They also note that these U values are slightly on the small side relative to experiment. This is consistent with the observation in Ref. S97 that the best description of the low-temperature ordered phase is obtained within LDA+ U with $U = 4$ eV. Kolorenč *et al.* add an interesting discussion of the differences in the treatment of screening in LDA+ U and LDA+Hubbard I. They argue that screening by ligand states is absent at the LDA+ U or LDA+Hubbard I levels such that the U used must already incorporate these screening processes. For LDA+DMFT, on the other hand, they argue that some screening comes in through the coupling of the f -states to a dynamical bath, requiring a larger U . Our cRPA calculations for the reduction of U by screening through the ligands agrees well with these estimates.

For completeness we note that there is an additional effect. U values will depend on the basis used with the two extremes being a set of localized atomic-like f - and p -orbitals and a block-diagonal basis where f - p hybridization enters effectively. We illustrate this on a simple two-orbital model with atomic-like f - and p -orbitals, hybridizing with strength V . The eigenvalues read, in terms of the energies of the local levels ϵ_f and $\epsilon_p = \epsilon_f - \Delta$ of the f and p state respectively:

$$E = \frac{1}{2}(\epsilon_f + \epsilon_p) \pm \frac{1}{2}\sqrt{(\epsilon_f - \epsilon_p)^2 + 4|V|^2} \quad (\text{S2})$$

and the eigenvectors can be expressed in terms of the atomic

states $|f\rangle, |p\rangle$:

$$|\pm\rangle = \cos(\theta)|f\rangle \pm \sin(\theta)|p\rangle \quad (\text{S3})$$

with $\tan(\theta) = -\frac{\Delta}{2V} + \sqrt{(\frac{\Delta}{2V})^2 + 1}$. Since U^{ff} transforms as $\cos(\theta)^4$, the values in an atomic-like basis are reduced when transforming to a basis that block diagonalizes the fp Hamiltonian. The precise amount of reduction depends on the orbitals since the hybridization is strongly orbital-dependent.

RELATION BETWEEN CLUSTER CALCULATIONS AND DMFT CALCULATIONS

The rewriting of the Hamiltonian presented in the main text of our paper also allows for a deeper understanding of the relation between cluster model calculations and DFT+DMFT. Indeed, by definition, the cluster model assumes the total particle number to be fixed to specific integer values, and diagonalizes the cluster Hamiltonian for those. In DMFT, in general, the bath introduces the possibility of charge fluctuations and the above assumption becomes less obvious. A cluster approximation for insulators is well justified since the bath hybridization is small. For metallic systems, restricting the Hamiltonian the low-energy correlated subspace avoids the problem. The Zhang-Rice-like construction presented above provides a way to do so explicitly. Otherwise, when the O p -states are to be kept explicitly in the description, the shifts induced by the changes in the particle number might have to be taken into account explicitly.

-
- [S1] F. Aryasetiawan, M. Imada, A. Georges, G. Kotliar, S. Biermann, and A. I. Lichtenstein, Phys. Rev. B **70**, 195104 (2004).
 - [S2] T. Miyake, F. Aryasetiawan, and M. Imada, Phys. Rev. B **80**, 155134 (2009).
 - [S3] E. Şaşıoğlu, C. Friedrich, and S. Blügel, Phys. Rev. B **83**, 121101 (2011).
 - [S4] B.-C. Shih, T. A. Abtew, X. Yuan, W. Zhang, and P. Zhang, Phys. Rev. B **86**, 165124 (2012).
 - [S5] T. Miyake and F. Aryasetiawan, Phys. Rev. B **77**, 085122 (2008).
 - [S6] J. M. Tomczak, T. Miyake, and F. Aryasetiawan, Phys. Rev. B **81**, 115116 (2010).
 - [S7] C. Martins, M. Aichhorn, L. Vaugier, and S. Biermann, Phys. Rev. Lett. **107**, 266404 (2011).
 - [S8] L. Vaugier, H. Jiang, and S. Biermann, Phys. Rev. B **86**, 165105 (2012).
 - [S9] R. Sakuma and F. Aryasetiawan, Phys. Rev. B **87**, 165118 (2013).
 - [S10] P. Werner, R. Sakuma, F. Nilsson, and F. Aryasetiawan, Phys. Rev. B **91**, 125142 (2015).
 - [S11] P. Werner, M. Casula, T. Miyake, F. Aryasetiawan, A. J. Millis, and S. Biermann, Nat. Phys. **8**, 331 (2012).
 - [S12] K. Nakamura, R. Arita, and M. Imada, J. Phys. Soc. Jpn. **77**, 093711 (2008).
 - [S13] T. Miyake, L. Pourovskii, V. Vildosola, S. Biermann, and A. Georges, J. Phys. Soc. Jpn. **77**, 99 (2008).
 - [S14] M. Imada and T. Miyake, J. Phys. Soc. Jpn. **79**, 112001 (2010).

- [S15] A. van Roekeghem, T. Ayril, J. M. Tomczak, M. Casula, N. Xu, H. Ding, M. Ferrero, O. Parcollet, H. Jiang, and S. Biermann, *Phys. Rev. Lett.* **113**, 266403 (2014).
- [S16] A. van Roekeghem et al., *in preparation*.
- [S17] K. Karlsson, F. Aryasetiawan, and O. Jepsen, *Phys. Rev. B* **81**, 245113 (2010).
- [S18] J. M. Tomczak, L. V. Pourovskii, L. Vaugier, A. Georges, and S. Biermann, *Proc. Natl. Acad. Sci. USA* **110**, 904 (2013).
- [S19] F. Nilsson, R. Sakuma, and F. Aryasetiawan, *Phys. Rev. B* **88**, 125123 (2013).
- [S20] Y. Nomura, K. Nakamura, and R. Arita, *Phys. Rev. B* **85**, 155452 (2012).
- [S21] K. Nakamura, Y. Yoshimoto, and M. Imada, *Phys. Rev. B* **86**, 205117 (2012).
- [S22] J. M. Tomczak, T. Miyake, R. Sakuma, and F. Aryasetiawan, *Phys. Rev. B* **79**, 235133 (2009).
- [S23] P. H. Dederichs, S. Blügel, R. Zeller, and H. Akai, *Phys. Rev. Lett.* **53**, 2512 (1984).
- [S24] O. Gunnarsson, O. K. Andersen, O. Jepsen, and J. Zaanen, *Phys. Rev. B* **39**, 1708 (1989).
- [S25] V. I. Anisimov and O. Gunnarsson, *Phys. Rev. B* **43**, 7570 (1991).
- [S26] M. Cococcioni and S. de Gironcoli, *Phys. Rev. B* **71**, 035105 (2005).
- [S27] S. Biermann, *J. Phys.: Condens. Mat.* **26**, 173202 (2014).
- [S28] H. Jiang, *Int. J. Quantum Chem.* **115**, 722 (2015).
- [S29] E. Wuilloud, H. R. Moser, W. D. Schneider, and Y. Baer, *Phys. Rev. B* **28**, 7354 (1983).
- [S30] D. M. Wieliczka, C. G. Olson, and D. W. Lynch, *Phys. Rev. B* **29**, 3028 (1984).
- [S31] B. Johansson, *Philos. Mag.* **30**, 469 (1974).
- [S32] J. W. Allen and R. M. Martin, *Phys. Rev. Lett.* **49**, 1106 (1982).
- [S33] J. W. Allen and L. Z. Liu, *Phys. Rev. B* **46**, 5047 (1992).
- [S34] M. Lavagna, C. Lacroix, and M. Cyrot, *Phys. Lett. A* **90**, 210 (1982).
- [S35] R. Sakuma, T. Miyake, and F. Aryasetiawan, *Phys. Rev. B* **86**, 245126 (2012).
- [S36] M. Casadei, X. Ren, P. Rinke, A. Rubio, and M. Scheffler, *Phys. Rev. Lett.* **109**, 146402 (2012).
- [S37] K. Held, A. K. McMahan, and R. T. Scalettar, *Phys. Rev. Lett.* **87**, 276404 (2001).
- [S38] M. B. Zöfl, I. A. Nekrasov, T. Pruschke, V. I. Anisimov, and J. Keller, *Phys. Rev. Lett.* **87**, 276403 (2001).
- [S39] A. K. McMahan, K. Held, and R. T. Scalettar, *Phys. Rev. B* **67**, 075108 (2003).
- [S40] K. Haule, V. Oudovenko, S. Y. Savrasov, and G. Kotliar, *Phys. Rev. Lett.* **94**, 036401 (2005).
- [S41] B. Amadon, S. Biermann, A. Georges, and F. Aryasetiawan, *Phys. Rev. Lett.* **96**, 066402 (2006).
- [S42] S. V. Streltsov, E. Gull, A. O. Shorikov, M. Troyer, V. I. Anisimov, and P. Werner, *Phys. Rev. B* **85**, 195109 (2012).
- [S43] M. S. Litsarev, I. Di Marco, P. Thunström, and O. Eriksson, *Phys. Rev. B* **86**, 115116 (2012).
- [S44] J. Bieder and B. Amadon, *Phys. Rev. B* **89**, 195132 (2014).
- [S45] N. Lanatà, Y.-X. Yao, C.-Z. Wang, K.-M. Ho, and G. Kotliar, *Phys. Rev. B* **90**, 161104 (2014).
- [S46] B. Chakrabarti, M. E. Pezzoli, G. Sordi, K. Haule, and G. Kotliar, *Phys. Rev. B* **89**, 125113 (2014).
- [S47] N. Devaux, M. Casula, F. Decremps, and S. Sorella, *Phys. Rev. B* **91**, 081101 (2015).
- [S48] R. Dong, X. Wan, X. Dai, and S. Y. Savrasov, *Phys. Rev. B* **89**, 165122 (2014).
- [S49] B. Amadon, T. Applencourt, and F. Bruneval, *Phys. Rev. B* **89**, 125110 (2014).
- [S50] J. Zaanen, G. A. Sawatzky, and J. W. Allen, *Phys. Rev. Lett.* **55**, 418 (1985).
- [S51] S. Hüfner, J. Osterwalder, T. Riesterer, and F. Hulliger, *Solid State Commun.* **52**, 793 (1984).
- [S52] G. A. Sawatzky and J. W. Allen, *Phys. Rev. Lett.* **53**, 2339 (1984).
- [S53] B. E. F. Fender, A. J. Jacobson, and F. A. Wedgwood, *J. Chem. Phys.* **48**, 990 (1968).
- [S54] A. K. Cheetham and D. A. O. Hope, *Phys. Rev. B* **27**, 6964 (1983).
- [S55] Z.-X. Shen, C. K. Shih, O. Jepsen, W. E. Spicer, I. Lindau, and J. W. Allen, *Phys. Rev. Lett.* **64**, 2442 (1990).
- [S56] Z.-X. Shen, R. S. List, D. S. Dessau, B. O. Wells, O. Jepsen, A. J. Arko, R. Bartlett, C. K. Shih, F. Parmigiani, J. C. Huang, et al., *Phys. Rev. B* **44**, 3604 (1991).
- [S57] Z.-X. Shen, R. S. List, D. S. Dessau, A. J. Arko, R. Bartlett, O. Jepsen, B. O. Wells, and F. Parmigiani, *Solid State Commun.* **79**, 623 (1991).
- [S58] A. Fujimori, F. Minami, and S. Sugano, *Phys. Rev. B* **29**, 5225 (1984).
- [S59] L. H. Tjeng, C. T. Chen, J. Ghijsen, P. Rudolf, and F. Sette, *Phys. Rev. Lett.* **67**, 501 (1991).
- [S60] J. Fink, N. Nücker, E. Pellegrin, H. Romberg, M. Alexander, and M. Knupfer, *J. Electron Spectrosc. Relat. Phenom.* **66**, 395 (1994).
- [S61] F. Aryasetiawan and O. Gunnarsson, *Phys. Rev. Lett.* **74**, 3221 (1995).
- [S62] X. Ren, I. Leonov, G. Keller, M. Kollar, I. Nekrasov, and D. Vollhardt, *Phys. Rev. B* **74**, 195114 (2006).
- [S63] D. Korotin, A. V. Kozhevnikov, S. L. Skornyakov, I. Leonov, N. Binggeli, V. I. Anisimov, and G. Trimarchi, *Eur. Phys. J. B* **65**, 91 (2008).
- [S64] J. Kuneš, V. I. Anisimov, S. L. Skornyakov, A. V. Lukoyanov, and D. Vollhardt, *Phys. Rev. Lett.* **99**, 156404 (2007).
- [S65] M. Karolak, G. Ulm, T. Wehling, V. Mazurenko, A. Poteryaev, and A. Lichtenstein, *J. Electron Spectrosc. Relat. Phenom.* **181**, 11 (2010).
- [S66] F. Manghi, *J. Phys.: Condens. Mat.* **26**, 015602 (2014).
- [S67] J. Schoenes, *J. Appl. Phys.* **49**, 1463 (1978).
- [S68] T. M. McCleskey, E. Bauer, Q. Jia, A. K. Burrell, B. L. Scott, S. D. Conradson, A. Mueller, L. Roy, X. Wen, G. E. Scuseria, et al., *J. Appl. Phys.* **113**, 013515 (2013).
- [S69] D. Gryaznov, E. Heifets, and E. Kotomin, *Phys. Chem. Chem. Phys.* **11**, 7241 (2009).
- [S70] E. Vathonne, Ph.D. thesis, U. Aix-Marseille (2014).
- [S71] X.-D. Wen, R. L. Martin, T. M. Henderson, and G. E. Scuseria, *Chem. Rev.* **113**, 1063 (2013).
- [S72] M.-T. Suzuki, N. Magnani, and P. M. Oppeneer, *Phys. Rev. B* **82**, 241103 (2010).
- [S73] K. N. Kudin, G. E. Scuseria, and R. L. Martin, *Phys. Rev. Lett.* **89**, 266402 (2002).
- [S74] L. E. Roy, T. Durakiewicz, R. L. Martin, J. E. Peralta, G. E. Scuseria, C. G. Olson, J. J. Joyce, and E. Guzewicz, *J. Comput. Chem.* **29**, 2288 (2008).
- [S75] J. H. Jefferson, H. Eskes, and L. F. Feiner, *Phys. Rev. B* **45**, 7959 (1992).
- [S76] L. F. Feiner, J. H. Jefferson, and R. Raimondi, *Phys. Rev. B* **53**, 8751 (1996).
- [S77] R. Raimondi, J. H. Jefferson, and L. F. Feiner, *Phys. Rev. B* **53**, 8774 (1996).
- [S78] F. C. Zhang and T. M. Rice, *Phys. Rev. B* **37**, 3759 (1988).
- [S79] J. C. Slater and G. F. Koster, *Phys. Rev.* **94**, 1498 (1954).
- [S80] M. W. Haverkort, M. Zwierzycki, and O. K. Andersen, *Phys. Rev. B* **85**, 165113 (2012).
- [S81] B. Dorado, B. Amadon, M. Freyss, and M. Bertolus, *Phys. Rev. B* **79**, 235125 (2009).

- [S82] H. Y. Geng, Y. Chen, Y. Kaneta, and M. Kinoshita, *Phys. Rev. B* **75**, 054111 (2007).
- [S83] H. Y. Geng, H. X. Song, K. Jin, S. K. Xiang, and Q. Wu, *Phys. Rev. B* **84**, 174115 (2011).
- [S84] S. Dudarev, M. Castell, G. Botton, S. Savrasov, C. Muggelberg, G. Briggs, A. Sutton, and D. Goddard, *Micron* **31**, 363 (2000).
- [S85] S. L. Dudarev, G. A. Botton, S. Y. Savrasov, Z. Szotek, W. M. Temmerman, and A. P. Sutton, *Phys. Status Solidi A* **166**, 429443 (1998).
- [S86] S. L. Dudarev, D. N. Manh, and A. P. Sutton, *Philos. Mag. B* **75**, 613 (1997).
- [S87] D. Gryaznov, E. Heifets, and D. Sedmidubsky, *Phys. Chem. Chem. Phys.* **12**, 12273 (2010).
- [S88] O. Gunnarsson, D. D. Sarma, F. U. Hillebrecht, and K. Schhammer, *J. Appl. Phys.* **63**, 3676 (1988).
- [S89] S. Hongliang, C. Mingfu, and Z. Ping, *J. Nucl. Mater.* **400**, 151 (2010).
- [S90] F. Jollet, T. Petit, S. Gota, N. Thromat, M. Gautier-Soyer, and A. Pasturel, *J. Phys.: Condens. Mat.* **9**, 9393 (1997).
- [S91] J. Kolorenč, A. B. Shick, and A. I. Lichtenstein, arXiv:1504.07979 (2015).
- [S92] A. Kotani and T. Yamazaki, *Prog. Theor. Phys. Supp.* **108**, 117 (1992).
- [S93] L. Petit, A. Svane, Z. Szotek, W. M. Temmerman, and G. M. Stocks, *Phys. Rev. B* **81**, 045108 (2010).
- [S94] J. H. Shim, K. Haule, and G. Kotliar, *Europhys. Lett.* **85**, 17007 (2009).
- [S95] Q. Yin, A. Kutepov, K. Haule, G. Kotliar, S. Y. Savrasov, and W. E. Pickett, *Phys. Rev. B* **84**, 195111 (2011).
- [S96] Q. Yin and S. Y. Savrasov, *Phys. Rev. Lett.* **100**, 225504 (2008).
- [S97] M.-T. Suzuki, N. Magnani, and P. M. Oppeneer, *Phys. Rev. B* **88**, 195416 (2013).